HEAT TRANSFER IN A TRIANGULAR WAVY CHANNEL WITH CuO-WATER NANOFLUIDS UNDER PULSATING FLOW

by

Unal AKDAG [a]*, Selma AKCAY [b], and Dogan DEMIRAL [a]

[a] Mechanical Engineering Department, Aksaray University, Aksaray, Turkey
[b] Institute of Science and Technology, Aksaray University, Aksaray, Turkey

Original scientific paper
https://doi.org/10.2298/TSCI161018015A

In this paper, heat transfer and pressure drop characteristics of CuO-water nanofluid flow in a isothermally heated triangular-wavy channel under pulsating inlet conditions are numerically investigated. A numerical simulation is conducted by solving the governing continuity, momentum, and energy equations for laminar flow using the finite volume approach. In the studies, the main parameters including the Reynolds number, pulsating amplitude and frequency, are changed while the nanoparticle volume fraction and the other parameters are kept constant for all cases. Numerical results are compared with the steady flow conditions, which showed that heat transfer performance significantly increases due to improve thermal conductivity and the use of nanoparticles in the pulsating flow conditions. The results indicate that there is a high potential for promoting the thermal performance enhancement by using nanoparticles under pulsating flow in wavy channels. It is found that the heat transfer enhancement increases with increasing pulsating amplitude and Reynolds number, and there is a slight increase in pressure drop. The obtained results are given as a function of dimensionless parameters.

Key words: *nanofluids, pulsating flow, triangular wavy-channel, heat transfer enhancement*

Introduction

In recent years, wavy channels of different geometries have been used to improve heat transfer in engineering applications, such as heat exchange. Wavy channels have potential to improve heat transfer. Heat transfer with conventional fluid in a wavy channel has been investigated experimentally and numerically by many researchers. Results of numerical and experimental investigations on the convective heat transfer in channels with wavy surface geometry indicated that due to providing a self-oscillating flow the heat transfer was considerably enhanced from that of straight channels, but with an increasing drop in pressure [1-5]. The effect of pulsatile flow in wavy channels was examined to further improve the heat transfer and fluid mixture [6-9]. Nandi and Chattopadhyay [10], using a sinusoidal wavy channel, and Jin *et al.* [11] using a triangular wavy channel, investigated the effect on the heat transfer of pulsating flow, and reported that depending on the pulsating parameters, a significant improvement in heat transfer could occur.

Another promising method used to increase the heat transfer in wavy channels is the addition of nanoparticles into the flow. Several numerical and experimental studies were

* Corresponding author, e-mail: uakdag@gmail.com

performed on the use of nanofluid to enhance heat transfer. It has been reported that adding nanoparticles to traditional heat transfer fluids can lead to improvement in their thermal conductivity [12-17]. Yang *et al.* [16], numerically studied the influences of the Reynolds number, the particle volume fraction, and the wavy channel amplitude on the heat transfer enhancement of nanofluids. They reported that the thermal enhancement achieved 24% in the wavy channel flow compared with pure fluid for a particle volume fraction of $\varphi = 5\%$ of Cu-water nanofluids. Heidary and Kermani [18], numerically studied laminar flow and heat transfer of nanofluids in a sinusoidal wavy channel. They investigated the effects of changing the Reynolds number, the nanoparticle volume fraction and the wavy amplitude on the flow and thermal characteristics. Their results showed that the addition of nanoparticles to the base fluid dramatically enhances the heat transfer in wavy channels. Naphon [19], experimentally investigated the heat transfer and pressure drop of triangular corrugated channel, and declared that the corrugated surface has significant effect on the enhancement of heat transfer and pressure drop. Ahmed *et al.* [20], numerically investigated laminar Cu-water nanofluid flow and heat transfer in a wavy channel. The Reynolds number and nanoparticle volume fraction considered were in the ranges of 100-800 and 0-5%, respectively. In their second paper, Ahmed *et al.* [21], numerically investigated heat transfer of Cu-water nanofluids in a trapezoidal-corrugated channel. The numerical results showed that the average Nusselt number increases with increasing nanoparticle volume fraction and amplitude of the corrugated channel.

In the pulsating flow conditions, the combined effect of pulsation and nanoparticles can improve the heat transfer as well as the mixing of fluids in wavy channels. The pulsating flow has the advantage of preventing sedimentation of nanoparticles in the base fluid, to provide strong mixing of nanoparticles near the wavy wall, leading to a better thermal performance. There are few studies that examined nanofluids with pulsating flow in wavy channels in literature [22]. The heat transfer characteristics of Al_2O_3-water based nanofluids in a wavy mini-channel under pulsating inlet flow conditions were investigated numerically by Akdag *et al.* [23]. They declared that there was a strong potential in promoting the thermal performance enhancement by using the nanoparticles under laminar pulsating flow. The numerical results indicated that the heat transfer performance increased significantly with increasing nanoparticle volume fraction and amplitude of pulsation. Akdag *et.al.* [24], numerically investigated the effect of CuO-water based nanofluids on the heat transfer in a trapezoidal corrugated channel under *laminar* pulsating inlet conditions. They showed that the heat transfer performance considerably increased with increasing pulsating amplitude at low frequencies compared with that in steady flow.

However, the literature review reveals that most of these studies were applied only for nanofluids flow inside wavy channels, and were not combined with pulsating flow. There are a few studies that of nanofluids with pulsating flow in wavy channels. Nevertheless, pulsation in nanofluids is not implemented in a triangular wavy channel in the literature. Therefore, in this paper, the convective heat transfer of CuO-water based nanofluids in a triangular wavy channel under pulsating inlet flow conditions is numerically investigated for different Reynolds numbers ($200 \leq Re \leq 700$) and a nanoparticle volume fraction of 5%. The numerical simulations are performed by solving the governing equations using the finite volume approach. The effects of the Reynolds number, pulsating frequency and amplitude on heat transfer performance are analyzed.

Numerical model

Description of the physical domain

Figure1 shows the basic geometry of the triangular wavy channel used in the present study. The geometry considered has an unheated straight section of 2λ at the inlet and outlet, and channel height, H, of 10 mm. The channel consists of eight wavy pieces.

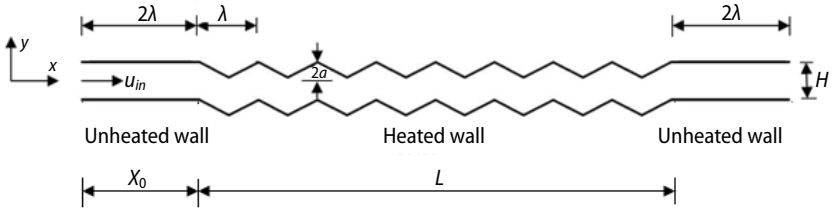

Figure 1. The geometry of the triangular wavy channel

The geometric parameters are kept constant, including the wave amplitude (a = 2 mm) and corrugated length (λ = 20 mm). The fluid is a suspension of CuO nanoparticles in water, and a nanoparticle volume fraction of φ = 5% is used.

Governing equations

It can be assumed that the flow is fully developed, laminar, incompressible, 2-D, and unsteady [25]. Additionally, the nanofluid is considered as a Newtonian fluid. The single phase flow is assumed by considering the local thermal equilibrium. The mixture of water and nanoparticles of CuO is homogenous and enters the channel under the same flow and thermal conditions. Gravity and radiation heat transfer are negligible. Therefore, the governing equations based on these assumptions are:

– continuity equation

$$\frac{\partial u}{\partial x}+\frac{\partial v}{\partial y}=0 \tag{1}$$

– momentum equations

$$\frac{\partial u}{\partial t}+u\frac{\partial u}{\partial x}+v\frac{\partial u}{\partial y}=-\frac{1}{\rho_{\mathrm{nf}}}\frac{\partial p}{\partial x}+\nu_{\mathrm{nf}}\left(\frac{\partial^2 u}{\partial x^2}+\frac{\partial^2 u}{\partial y^2}\right) \tag{2}$$

$$\frac{\partial v}{\partial t}+u\frac{\partial v}{\partial x}+v\frac{\partial v}{\partial y}=-\frac{1}{\rho_{\mathrm{nf}}}\frac{\partial p}{\partial y}+\nu_{\mathrm{nf}}\left(\frac{\partial^2 v}{\partial x^2}+\frac{\partial^2 v}{\partial y^2}\right) \tag{3}$$

– energy equation

$$\frac{\partial T}{\partial t}+u\frac{\partial T}{\partial x}+v\frac{\partial T}{\partial y}=\alpha_{\mathrm{nf}}\left(\frac{\partial^2 T}{\partial x^2}+\frac{\partial^2 T}{\partial y^2}\right) \tag{4}$$

where ρ_{nf}, ν_{nf} and α_{nf} ($\alpha_{\mathrm{nf}} = k_{\mathrm{nf}}/\rho_{\mathrm{nf}}C_{\mathrm{nf}}$) denote the density, kinematic viscosity, and thermal diffusivity of the nanofluid, respectively.

Boundary conditions

The fluid enters the channel with uniform temperature T_0 = 293 K. At the channel inlet, the velocity profile is found by adding the uniform velocity profile with a sinusoidal pulsation. The sinusoidal pulsating velocity profile is given:

$$u_{\text{in}} = U_{\text{o}}\left[1 + A_{\text{o}}\sin(\omega t)\right] \tag{5}$$

where A_{o} is the non-dimensional amplitude ($A_{\text{o}} = x_m/H$), ω – the angular frequency and the non-dimensional frequency is defined as the Womersley number, where Wo = $H/2(\omega/\nu)^{1/2}$, and ν is the kinematic viscosity of the inlet flow. The inlet boundary conditions are given:

$$u = u_{\text{in}}, \quad v = 0, \quad T_0 = 293\ \text{K} \tag{6}$$

The flow at the outlet is assumed fully developed and is applied following the boundary conditions.

$$\frac{\partial u}{\partial x} = \frac{\partial v}{\partial x} = 0, \quad \frac{\partial T}{\partial x} = 0 \tag{7}$$

Isothermal conditions are applied at all triangular wavy channel walls. Both the top and bottom wavy surfaces are kept at an isothermal temperature of 330 K. The no-slip boundary conditions are applied along the corrugated channel walls:

$$u = v = 0, \quad T_w = 330\ \text{K} \tag{8}$$

The no-slip boundary condition and adiabatic wall boundary conditions are defined along the unheated straight inlet and outlet section of the channel.

$$u = v = 0, \quad \frac{\partial T}{\partial n} = 0 \tag{9}$$

In this study, the problem is solved dimensionally with relevant boundary conditions, and the results are given as a function of the dimensionless parameters.

Numerical method and grid testing

The control volume based commercial CFD code FLUENT [26] is utilized to solve the governing equations. The computational domain is generated by using the preprocessing code GAMBIT. Un-structured cells are used to mesh the domain. For discretization of the momentum and energy equations, the second order upwind scheme is applied. The SIMPLE algorithm is selected as the pressure-velocity coupling scheme. Interpolation of pressure is performed by the standard scheme, which uses the coefficient from the momentum equation to calculate the pressure at the faces of the discretized volume. For applying the pulsating inlet velocity, a user-defined function (udf) is written. The under-relaxation for velocity, pressure and temperature is performed to achieve the convergence of the numerical solution. The convergence criterion for energy equation and each variable is determined to be 10^{-6}.

The mesh is finer near the walls to resolve the high gradients in the thermal and hydrodynamic boundary-layer. For grid independency, it is conducted to obtain an optimal grid distribution with accurate results over a minimum computational time. To test the grid independence, the number of cells was varied, *i. e.*, 30 × 420, 40 × 500, 50 × 600, 60 × 600, and 60 × 720, in various steps. After 50 × 600 grids, a further increase in the cells was found to have less than 2% variation in the Nusselt number. Typically, the 50 × 600 grid was used in triangular

wavy channel. The numerical solution parameters are given in tab. 1.

Table 1. Numerical solution parameters

Reynolds number	Amplitude A_o	Frequency Wo
200	0.5, 0.8, 1	3, 4, 6, 9, 14
500	0.5, 0.8, 1	3, 4, 6, 9, 14
700	0.5, 0.8, 1	3, 4, 6, 9, 14

Physical properties of the nanofluids

The working fluid is water with CuO nanoparticles. The thermophysical properties of nanofluid include thermal conductivity, viscosity, density and heat capacitance depending on what form the governing equations are written. By assuming the nanoparticles are well dispersed within the base fluid, the effective thermophysical properties of the nanofluids can be evaluated using some classical appropriate formulas. The effective thermophysical properties of nanofluids are defined using the following formulas:

The density and specific heat of the nanofluid are calculated using the Pak and Cho [27] correlations, which are defined:

$$\rho_{\mathrm{nf}} = (1-\varphi)\rho_{\mathrm{bf}} + \varphi\rho_{\mathrm{pt}} \tag{10}$$

$$C_{\mathrm{nf}} = (1-\varphi)C_{\mathrm{bf}} + \varphi C_{\mathrm{pt}} \tag{11}$$

Dynamic viscosity of the nanofluid is calculated using the correlation obtained from the least square curve fitting of the experimental data of Wang *et al.* [28]

$$\mu_{\mathrm{nf}} = \mu_{\mathrm{bf}}(123\varphi^2 + 7.3\varphi + 1) \tag{12}$$

The effective thermal conductivity of fluid has been determined by the model proposed by Patel *et al.* [29]. For the two-component entity of the spherical-particle suspension, the model gives:

$$\frac{k_{\mathrm{eff}}}{k_{\mathrm{bf}}} = 1 + \frac{k_{\mathrm{pt}}A_{\mathrm{pt}}}{k_{\mathrm{bf}}A_{\mathrm{bf}}} + Ck_{\mathrm{pt}}\,\mathrm{Pe}\frac{A_{\mathrm{pt}}}{k_{\mathrm{bf}}A_{\mathrm{bf}}} \tag{13}$$

where

$$\frac{A_{\mathrm{pt}}}{A_{\mathrm{bf}}} = \frac{d_{\mathrm{bf}}}{d_{\mathrm{pt}}}\frac{\varphi}{(1-\varphi)} \tag{14}$$

and

$$\mathrm{Pe} = \frac{u_{\mathrm{pt}}d_{\mathrm{pt}}}{\alpha_{\mathrm{bf}}} \tag{15}$$

where u_{pt} is the Brownian motion velocity of the particles, which is given:

$$u_{\mathrm{pt}} = \frac{2k_bT}{\pi\mu_{\mathrm{bf}}d_{\mathrm{pt}}^2} \tag{16}$$

where k_b is the Boltzmann constant. The calculation of effective thermal conductivity can be obtained from eq. (13). The diameter of the nanoparticles is 30 nm [17].

The subscripts *pt* and *bf* represent the nanoparticle and base fluids, respectively. Further details about the thermophysical properties of nanofluids are available in the literature [30-33]. The properties of CuO nanoparticles are given in tab. 2.

Table 2. Thermophysical properties of nanoparticles and the base fluid [17]

Material	ρ [kgm^{-3}]	C_p [Jkg^{-1}K^{-1}]	k [Wm^{-1}K^{-1}]	μ [kgm^{-1}s^{-1}]
Water	996.5	4181	0.613	0.001
CuO	6500	533	17.65	-

Results and discussion

The present study is validated by comparing the results obtained for nanoparticle volume fraction of $\varphi = 5\%$ and $100 \leq Re \leq 800$ with the numerical results of Ahmed *et al.* [17]. They numerically studied laminar forced convection heat transfer of CuO-water nanofluids in a triangular-corrugated channel. A similar geometry was simulated for the purpose of validating this study. In fig. 2(a) the comparison between the two sets of results show strong agreement. Ahmet *et al.* [17] is validated with the numerical results of Heidary and Kermani [18]. Also, the present study is validated by comparing the results obtained with the experimental results of Naphon [19]. They experimentally investigated laminar forced convection heat transfer in a triangular-corrugated channel for the constant heat flux $q'' = 0.58$ kW/m^2, wavy angle = 20° and $600 \leq Re \leq 1400$. A similar geometry was simulated for the purpose of validating this study. In fig. 2(b) the comparison between the two sets of results show strong agreement.

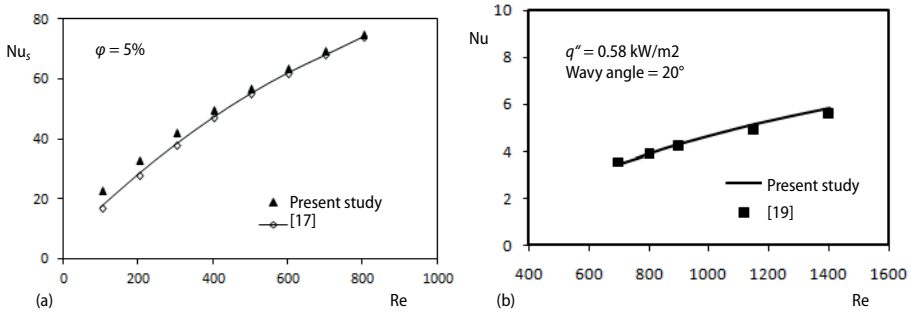

Figure 2. Verification of the present study, with [17], and [19]

In this section, the heat transfer mechanism is discussed using the pulsating flow in the wavy channel by examining the effects of various parameters. Geometric parameters of the wavy channel are kept constant for all cases. The three main parameters affecting the heat transfer characteristics in the triangular wavy channel are amplitude, A_o, frequency, Wo, and Reynolds number. These parameters are more important in the convection of pulsating flow. The simulations are focused on the behavior of the unsteadiness affecting the heat transfer mechanism. In this situation, due to the pulsating component, a periodic flow field was observed in the channel, and heat transfer was achieved periodically. Therefore, the heat transfer calculations are performed according to the amount of heat transfer achieved during one period of pulsation. In other words, the flow is assumed to be time periodic. To explain how the mechanisms behave over a cycle, phase angles have been used and presented by $\tau = \omega t$. The 2π radian or 360° indicates a cycle. The results are evaluated after the system achieved full periodic state. To explain the heat transfer mechanism, the instantaneous velocity and temperature distributions are obtained.

It may also be important to discuss of the flow regimes in the wavy channels. The transition of laminar to turbulence is strongly dependent on the geometry and fluid properties in the wavy channels. Rush *et al.* [34] are given a literature survey about transition of flow in wavy channels. In generally, the flow will become transition from laminar to turbulent after the Re = 1100 while the fully turbulence occurs about $Re \geq 1800$ for the wavy channel. On the

other hand, Das and Arakeri [35] has been investigated the criteria to ascertain the onset of transition in straight ducts by using Reynolds number based on the Stokes layer thickness, $\delta = (2\nu/\omega)^{1/2}$. They found that the no transition to turbulence occurs for $\mathrm{Re}_\delta < 1200$. However, most work addressing the onset of transition whether through laminar unsteadiness or turbulence considers only fully developed periodic flows [36, 37]. Therefore, the present study can be assumed fully developed laminar time periodic flow.

In the present study, laminar forced convection flow of CuO-water nanofluid in a wavy channel under pulsating flow conditions is numerically investigated. The geometric parameters and nanoparticle volume fraction (φ = 5%) are fixed, and the Reynolds number and pulsating parameters are changed. Due to the agglomeration and sedimentation problem, the volume fraction of nanoparticles has been selected as the maximum value of 5% [32, 33]. The frequency of pulsating flow is varied in the range of $3 \leq \mathrm{Wo} \leq 14$ for three pulsating amplitudes of A_o = 0.5, 0.8, and 1. The Reynolds number is set as 200, 500, and 700.

The temperature contours and vorticity magnitudes for different Reynolds numbers at a constant frequency (Wo = 6), constant amplitude (A_o = 1) and constant nanoparticle volume fraction (φ = 5%), with a 90° phase angle are shown in fig. 3(a) and 3(b), respectively. The temperature fields and flow structure are changed along the wavy channel by pulsations with varying Reynolds numbers. It is observed that the temperature and vorticity contours are symmetric about the axial direction for all values of Reynolds number. Additionally, it is observed that from the vorticity contours, reversal flow occurs in cavities of the wavy channel. The increase of pulsating inlet velocity increases the flow oscillations into the channel. This leads to the formation of the re-circulation regions near the upper and lower walls of the cavities. The pulsating effect contributes to the occurrence of a strong vortex in the cavities, which causes the increase of fluid mixing and improves the convective effect. It can be observed from the temperature

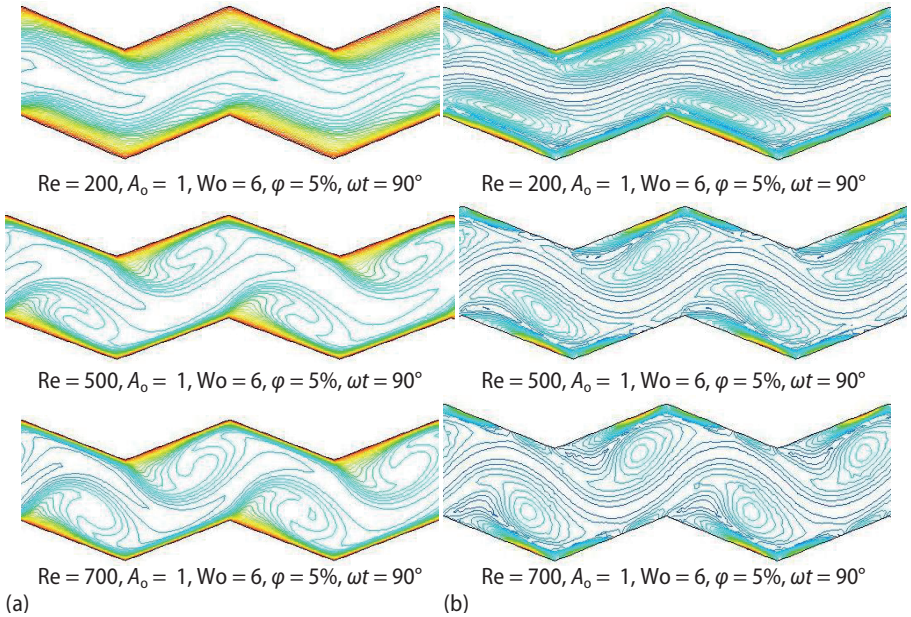

Figure 3. (a) Temperature contours for different Reynolds numbers at a fixed frequency, amplitude and specific phase angle, (b) vorticity magnitude for the conditions in fig. 3(a) (*for color image see journal web site*)

contours that the thickness of the thermal boundary-layer decreases and the temperature gradient at the walls of channels increase with increasing Reynolds number. This is because the re-circulation regions generated in such channels can improve the mixing of cold fluid in cores with hot fluid close to the walls of the corrugated-channels. The cold fluid had better contact to the wavy wall surfaces at high Reynolds numbers, which caused it to cool more quickly and therefore, the heat transfer enhancement increased.

The temperature contours and vorticity magnitudes for one cycle at a fixed Reynolds number (Re = 700), pulsating amplitude (A_o = 1), pulsating frequency (Wo = 6), and nanoparticle volume fraction (φ = 5%) are presented in figs. 4(a) and 4(b). In these figures, the temperature fields and vorticity structures change significantly depending on the phase angles. The fluid mixture improves due to contact between the heated wavy walls and cold fluid, which repeats periodically and causes an increase in the heat transfer enhancement.

The temperature contours and vorticity magnitudes for different frequencies at a fixed Reynolds number (Re = 700), pulsating amplitude (A_o = 1), and nanoparticle volume fraction (φ = 5%) with a phase angle of 270° are presented in figs. 5(a) and 5(b). The pulsating frequency substantially affected the temperature and flow fields, these flow structures were more pronounced, especially at low frequency, but this effect was reduced at high frequencies. The

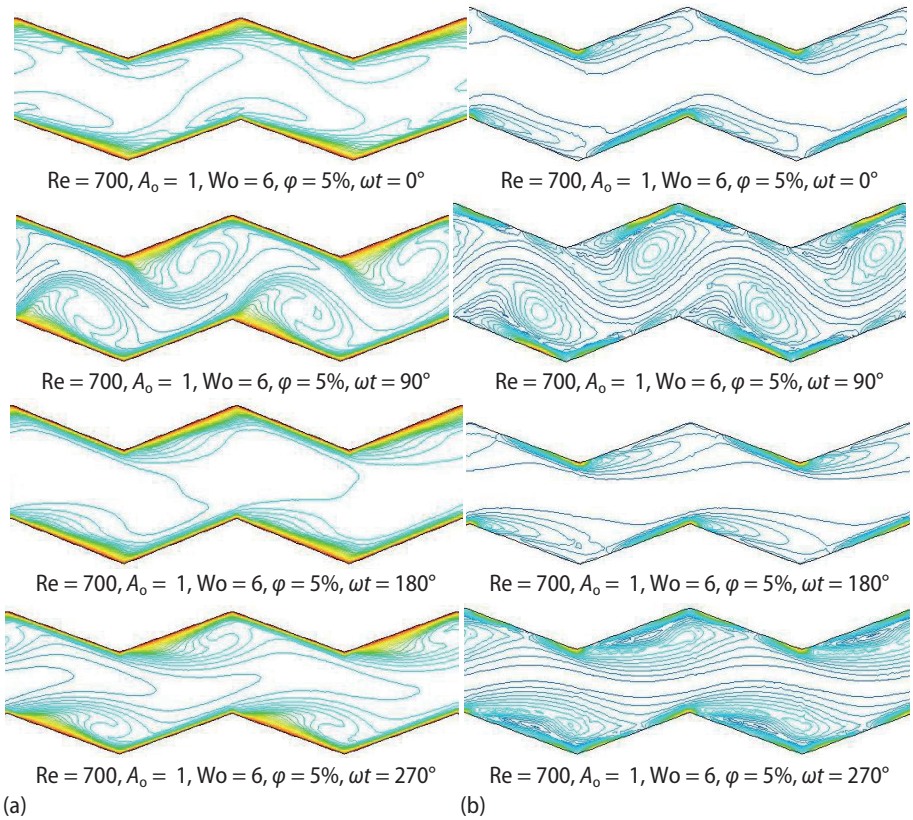

Figure 4. (a) Temperature contours at fixed amplitude, frequency and volume fraction over a cycle for Re = 700, (b) vorticity magnitude for conditions in fig. 4(a)
(*for color image see journal web site*)

temperature field is changed along the wavy channel by pulsating flow compared to the steady flow case. Because of the fluctuation effect of pulsating flow and the wavy channel geometry, strong vorticity is produced. This causes the large circulation region in the cavities, and which leads to the strong mixing in the flow field along the channel. The cold fluid is diffused to the heated wavy wall region and thus, heat transfer is enhanced remarkably. From these figures, the

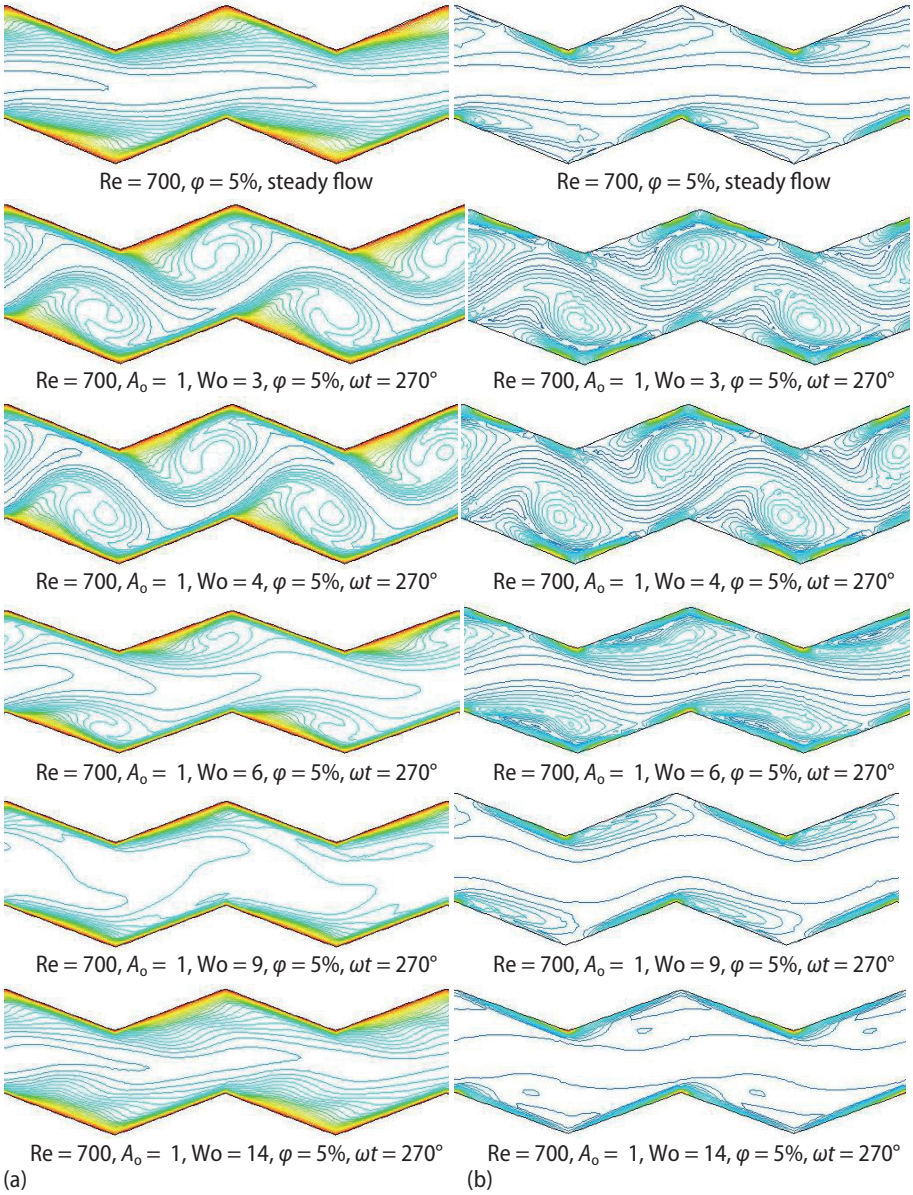

Figure 5. (a) Temperature contours at different frequencies at a fixed amplitude, phase angle and volume fraction for Re = 700, (b) vorticity magnitude for conditions in fig. 5(a) (*for color image see journal web site*)

velocity field is significantly affected at low frequency (Wo = 3, Wo = 4, Wo = 6) compared to that in steady flow. The higher frequencies do not contribute to enhancement of heat transfer.

Heat transfer calculation

To calculate the heat transfer, the flow and temperature fields are obtained, which are then used to calculate the Nusselt number as follows. The local and instantaneous Nusselt number for the corrugated wall is defined [25]:

$$\mathrm{Nu}_{x,t} = -\frac{k_{\mathrm{nf}}}{k_{\mathrm{bf}}}\left.\frac{\partial T}{\partial y}\right|_{x,t} \tag{17}$$

In this case, the time-averaged local Nusselt number is obtained by integrating the local Nusselt number over the walls of the corrugated channel as follows:

$$\mathrm{Nu}_t = \frac{1}{\tau}\int_0^{\tau} \mathrm{Nu}_{x,t}\,\mathrm{d}t \tag{18}$$

where τ is the time of the cycle, and L is the heated wall length. The space-averaged local Nusselt number is defined:

$$\mathrm{Nu}_x = \frac{1}{L}\int_{x_0}^{x_o+L} \mathrm{Nu}_{x,t}\,\mathrm{d}x \tag{19}$$

The overall heat transfer coefficient is obtained by an integration of the local and instantaneous Nusselt number over a cycle for a heated wall of wavy channels. For this purpose, the time-averaged Nusselt and space-averaged Nusselt numbers are combined with each other, and the total or cycle-averaged Nusselt number is defined:

$$\mathrm{Nu}_{\mathrm{p}} = \frac{1}{\tau L}\int_{x_o}^{x_o+L}\int_0^{\tau} \mathrm{Nu}(x,t)\mathrm{d}t\mathrm{d}x \tag{20}$$

where x_o is the unheated initial straight section of the channel. The effectiveness of the heat transfer is obtained by the heat transfer enhancement factor, ε, which is defined by eq. (21):

$$\varepsilon = \frac{\mathrm{Nu}_{\mathrm{p}}}{\mathrm{Nu}_{\mathrm{s}}} \tag{21}$$

where Nu_{p} is the cycle-averaged Nusselt number, eq. (20), Nu_{s} is the Nusselt number for steady flow (no pulsating flow for $\varphi = 5\%$). Thus, a value of ε over 1.0 denotes enhanced heat transfer. The variations of heat transfer performance with the dimensionless parameters in the wavy channel for fixed nanoparticle volume fracture ($\varphi = 5\%$) are shown in fig. 6.

In fig. 6(a), heat transfer performance *vs.* pulsating frequency with varying pulsating amplitude is presented at a fixed Reynolds number (Re = 200) and nanoparticle volume fraction ($\varphi = 5\%$). It is observed that there is an optimum Womersley number at which heat transfer enhancement is maximized. The maximum heat transfer enhancement is close to 40% according to steady flow at Wo = 4. The results reveal that the heat transfer performance decreases as frequency increases after the peak value of frequency for all amplitudes of pulsation. Heat transfer performance remained constant after a specific frequency (Wo = 6).

In fig. 6(b), the heat transfer performance *vs.* pulsating frequency with varying pulsating amplitudes is presented at a fixed Reynolds number (Re = 500) and nanoparticle vol-

ume fraction (φ = 5%). The results show that the heat transfer performance increases with the specific parameters of pulsation. As shown in the figure, the best heat transfer performance is found at low frequency and high amplitude. There is an optimum frequency at which the heat transfer enhancement is maximized. This is because when the flow frequency is low, the ratio of fluid residence time over the hot cavity to the heat diffusion time is high, allowing more heat to diffuse per unit of volumetric flow. The depth of heat penetration into the fluid increases during this period. The interaction of re-circulation with the core flow influences the temperature field and contributes to the increase of heat transfer. It is observed that the maximum heat transfer enhancement is close to 50% according to the steady flow at Wo = 6. The results reveal that the heat transfer performance decreases as frequency increases after the peak value of frequency for all amplitudes of pulsation.

In fig. 6(c) heat transfer performance *vs.* pulsating frequency with varying pulsating amplitude is presented at a fixed Reynolds number (Re = 700). The results show that the heat transfer performance increases as the pulsating amplitude increases. This is because there is sufficient time for growth of the vortex in cavities at low frequency, and the mixing of fluid in the wavy channel is improved. Therefore, the heat transfer is increased high amplitude and low frequency. A peak occurs at a specific value of frequency for each of pulsating amplitude. It is found that the maximum heat transfer enhancement is close to 60% for Wo = 6 according to the steady flow. The results show that the heat transfer performance decreases as frequency increases after the peak value of frequency for all amplitudes of pulsation.

It can be summarized that, the Reynolds number significantly affected the heat transfer performance. A peak occurs at a specific value of frequency for each of Reynolds number. As the Reynolds number increases, this peak shifts to the right. Heat transfer performance decreased after the peak value for each of Reynolds number. The best performance is obtained at a frequency of Wo = 6, for Re = 700. The results reveal that the heat transfer is significantly affected by pulsating flow parameters and the Reynolds number according to the steady flow case. There is an enhancement in heat transfer for all pulsating flow conditions compared with steady flow. This research is performed to verify the effect of pulsating flow with nanofluids on heat transfer enhancement and to investigate the mechanism of heat transfer by pulsating flow agitation in a triangular shaped wavy channel.

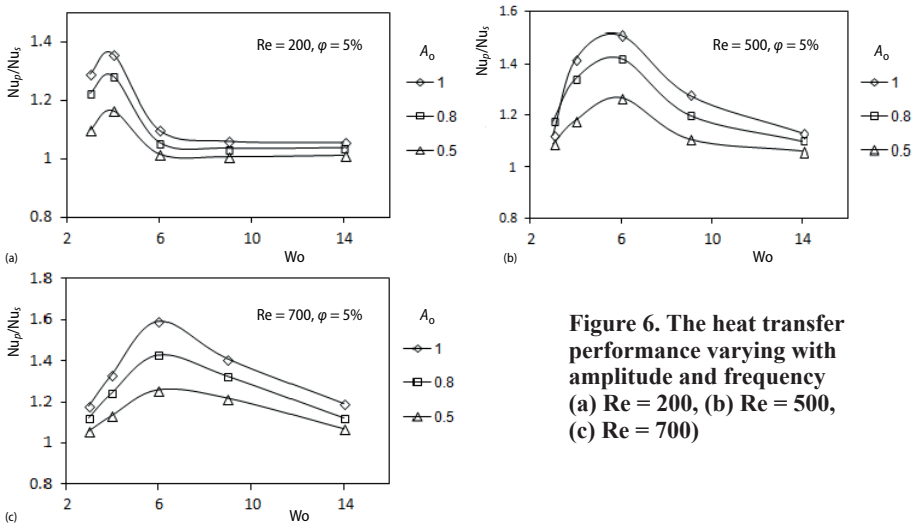

Figure 6. The heat transfer performance varying with amplitude and frequency (a) Re = 200, (b) Re = 500, (c) Re = 700)

Pressure drop calculation

Although there have been satisfactory results for heat transfer enhancement, the effects of pressure drop are an important subject in wavy channels under pulsating flow. The wavy walls and particle concentration contribute to a significant increase in the shear stress because of the interaction and collision among particles, fluid and the flow passage surfaces. It has been clearly shown in the literature that the addition of nanoparticles into a base fluid has produced an adverse effect on the wall shear stress. The nanoparticles increase the viscosity of the suspension. This is due to the nanofluids having a higher viscosity value in comparison with base fluids.

For the evaluation of pressure drop in the present wavy channel, the relative skin friction ratio is defined as $r = f_p/f_s$, where f_p is the average friction of the pulsating flow and f_s is the steady flow friction. The variation of friction for the dimensionless pulsating parameters at a fixed Reynolds number (Re = 700) and volume concentration with respect to the dimensionless amplitude and frequency is plotted in fig. 7. In this study, the skin friction results exhibit different behaviors depending on the heat transfer performance.

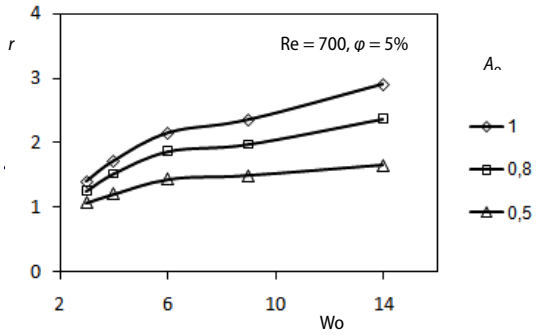

Figure 7. The relative skin friction varying with pulsating parameters (Re = 700)

From this investigation, it is found that the relative friction ratio increases with an increase in amplitude of pulsation. The increasing amplitude also increases the fluctuation effect in the flow, and as a result, the friction increases. In particular, the friction increases at low frequencies in the range of $3 < Wo < 6$, and when Wo = 6, the relative friction slightly changes with frequency at low pulsating amplitude. However, the relative friction also increases considerably as pulsating amplitude increases with the increase of frequency. It can be concluded that the pulsations and cavities contribute to the fluctuation effect in the flow, which causes the increase of the relative friction. The maximum heat transfer is obtained at low frequency (Wo = 6) and the highest Reynolds number (Re = 700), while there is a slight increase in pressure drop. For this frequency, the relative friction is more than two times that of the steady flow for higher amplitudes, as shown in fig. 7. It is reasonable for this parameter because the obtained heat transfer performance is greater than 60%.

In addition, it is interesting the note that, the pulsating flow and triangular wavy channel have an advantage in preventing the sedimentation of nanoparticles in nanofluid suspensions. This can be very important when using high volume concentrations of nanofluids in practical applications.

Conclusions

In this study, the effect of CuO-water based nanofluids on heat transfer in a triangular wavy channel under laminar pulsating inlet flow conditions is investigated numerically by using a control volume based CFD solver. For a specific nanoparticle volume ratio (φ = 5%) the effects of the Reynolds number, pulsation frequency and amplitude on the heat transfer enhancement are analyzed. In addition, the frictional pressure drop results are presented. The results show that the heat transfer performance considerably increased with increasing pulsat-

ing amplitude at low frequencies compared with that in steady flow. The combined effect of pulsations and nanoparticles in the wavy channel is favorable for increasing the Nusselt number compared to the steady flow case. This causes strong mixing between the hot fluid near the wavy wall and cold fluid in the main flow. As a result, the pulsating velocity of nanofluid has a considerable influence on the flow structure and thermal fields in the wavy channel, which may lead to heat transfer enhancement. The best heat transfer performance is obtained at Wo = 6, A_o = 1 and Re = 700. Substantial heat transfer enhancement can be obtained (ε up to 60%) in pulsating flows with low pulsating frequency, high amplitude and high Reynolds number. Therefore, these conditions can be proposed to achieve better performance and design more compact thermal devices.

Nomenclature

A_o – dimensionless pulsation amplitude
a – wavy wall amplitude, [m]
C – specific heat, [Jkg^{-1}K^{-1}]
C_p – specific heat, [Jkg^{-1}K^{-1}]
d – particle diameter, [m]
f – skin friction
H – channel height (characteristic length), [m]
k – conductivity, [Wm^{-1}K^{-1}]
L – heated wall length, [m]
Nu – Nusselt number.(= hL/k)
p – pressure, [Pa]
Pr – Prandtl number
Pe – Peclet number. (= RePr)
Re – Reynolds number. (= Ud_h/ν)
r – pressure drop ratio
T – temperature, [K]
T_w – wavy wall temperature, [K]
u, v – velocity components, [ms^{-1}]
U_o – average inlet velocity, [ms^{-1}]
u_{in}, U_{in} – instantaneous inlet velocity, [ms^{-1}]
Wo – Womersley number, [= $H/2(\omega/\nu)^{1/2}$]
t – time, [s]
x, y – Cartesian co-ordinates, [m]
x_m – amplitude of pulsation, [m]
x_o – unheated starting length, [m]

Greek Symbols

α – thermal diffusivity, [m^{-2}s]
ε – enhancement ratio
λ – corrugated cavity length, [m]
μ – dynamic viscosity, [kgm^{-1}s^{-1}]
ν – kinematic viscosity, [m^{2}s^{-1}]
ρ – fluid density, [kgm^{-3}]
τ – cycle time, ($\tau = \omega t$)
φ – volume fraction of particles, [%]
ω – angular frequency, (= $2\pi f$), [rads^{-1}]
ωt – phase angle

Subscripts

bf – base fluid
nf – nanofluid
p – pulsating
pt – particle
s – steady
w – wall

References

[1] Islamoglu, Y., Parmaksizoglu, C., The Effect of Channel Height on the Enhanced Heat Transfer Characteristics in a Corrugated Heat Exchanger Channel, *Appl.Thermal Engineering*. *23* (2003), 8, pp. 979-987
[2] Kruse, N., Rohr, P. R., Structure of Turbulent Heat Flux in a Flow over a Heated Wavy Wall, *Int. J. Heat Mass Transfer*, *49* (2006), 19-20, pp. 3514-3529
[3] Naphon, P., Heat Transfer Characteristics and Pressure Drop in Channel with V Corrugated Upper and Lower Plates, *Energy Conversion and Management, 48* (2007), 5, pp. 1516-1524
[4] Naphon, P., Kornkumjayrit, K., Numerical Analysis on the Fluid Flow and Heat Transfer in the Channel with V- Shaped Wavy Lower Plate, *Int. Commun. Heat Mass Transfer*, *35* (2008), 7, pp. 839-843
[5] Deylami, H. M., *et al*., Numerical Investigation of Heat Transfer and Pressure Drop in a Corrugated Channel, *International Journal of Engineering Transactions A: Basics*, *26* (2013), 7, pp. 771-780
[6] Nishimura, T., Kojima, N., Mass Transfer Enhancement in a Symmetric Sinusoidal Wavy-Walled Channel for Pulsatile Flow, *Int. J. Heat Mass Transfer*, *38* (1995), 9, pp. 1719-1731
[7] Lee, B. S.,*et al*., Chaotic Mixing and Mass Transfer Enhancement by Pulsatile Laminar Flow in a Axisymmetric Wavy Channel, *Int. J. Heat Mass Transfer*, *42* (1999), 14, pp. 2571-2581
[8] Jafari, M., *et al*., Pulsating Flow Effects on Convection Heat Transfer in a Corrugated Channel: A LBM Approach, *Int. Commun. Heat Mass Transfer*, *45* (2013), July, pp. 146-154

[9] Nandi, T. K., Chattopadhyay, H., Numerical Investigations of Developing Flow and Heat Transfer in Raccoon Type Microchannels under Inlet Pulsation. *Int. Commun. Heat Mass Transfer*, *56* (2014), Aug., pp. 37-41
[10] Nandi, T. K., Chattopadhyay, H., Numerical Investigations of Simultaneously Developing Flow in Wavy Microchannels under Pulsating Inlet Flow Condition, *Int. Commun. Heat Mass Transfer, 47* (2013), Oct., pp. 27-31
[11] Jin, D. X., *et al*., Effects of the Pulsating Flow Agitation on the Heat Transfer in a Triangular Grooved Channel, *Int. J. Heat Mass Transfer*, *50* (2007), 15-16, pp. 3062-3071
[12] Heris, S. Z., *et al*., Convective Heat Transfer of a Cu/Water Nanofluid Flowing through a Circular Tube, *Experimental Heat Transfer*, *22* (2009), 4, pp. 217-227
[13] Darzi, A. A. R., *et al*., Heat Transfer and Flow Characteristics of Al_2O_3-Water Nanofluid in a Double Tube Heat Exchanger, *Int. Commun. Heat Mass Transfer*, *47* (2013), Oct., pp. 105-112
[14] Vermahmoudi, Y., *et al*., Experimental Investigation on Heat Transfer Performance of Fe_2O_3/Water Nanofluid in an Air-Finned Heat Exchanger, *European Journal of Mechanics B/Fluids*, *44* (2014), Mar.,-Apr., pp. 32-41
[15] Sundar, L. S., Singh, M. K., Convective Heat Transfer and Friction Factor Correlations of Nanofluid in a Tube and with Inserts: A review, *Renewable and Sustainable Energy Reviews*, *20* (2013), Apr., pp. 23-35
[16] Yang, Y. T., *et al*., Numerical Optimization of Heat Transfer Enhancement in a Wavy Channel Using Nanofluids, *Int. Commun. Heat Mass Transfer*, *51* (2014), Feb., pp. 9-17
[17] Ahmed, M. A., *et al*., Effect of Corrugation Profile on the Thermal-Hydraulic Performance of Corrugated Channels Using CuO-Water Nanofluid, *Case Studies in Thermal Engineering*, *4* (2014), Nov., pp. 65-75
[18] Heidary, H., Kermani, M. J., Effect of Nano-Particles on Forced Convection in Sinusoidal-Wall Channel, *Int. Commun. Heat Mass Transfer*, *37* (2010), 10, pp. 1520-1527
[19] Naphon, P., Laminar Convective Heat Transfer and Pressure Drop in the Corrugated Channels, *International Communications in Heat and Mass Transfer*, *34* (2007), 1, pp. 62-71
[20] Ahmed, M. A., *et al*., Numerical Investigations on the Heat Transfer Enhancement in a Wavy Channel Using Nanofluid, *Int. J. Heat Mass Transfer*, *55* (2012), 21-22, pp. 5891-5898
[21] Ahmed, M. A., *et al*., Effects of Geometrical Parameters on the Flow and Heat Transfer Characteristics in Trapezoidal-Corrugated Channel Using Nanofluid, *Int. Commun. Heat Mass Transfer*, *42* (2013), Mar., pp. 69-74
[22] Rahgoshay, M., *et al*., Laminar Pulsating Flow of Nanofluids in a Circular Tube with Isothermal Wall, *Int. Commun. Heat Mass Transfer*, *39* (2012), 3, pp. 463-469
[23] Akdag, U., *et al*., Heat Transfer Enhancement with Laminar Pulsating Nanofluid Flow in a Wavy Channel, *Int. Commun. Heat Mass Transfer*, *59* (2014), Dec., pp. 17-23
[24] Akdag, U., *et al*., Numerical Investigation of Heat Transfer Enhancement with Nanofluids under Laminar Pulsating Flow in a Trapezoidal-Corrugated Channel, *Proceedings*, 15th Int. Conference on Advances in Mechanical Engineering, 2015, Istanbul, Turkey, (inCD) p. 921
[25] Ahmed, M. A., *et al*., Numerical Investigations of Flow and Heat Transfer Enhancement in a Corrugated Channel Using Nanofluid *Int. Commun. Heat Mass Transfer, 38* (2011), 10, pp. 1368-1375
[26] ***, Fluent 6.3. FLUENT User's Guide, Fluent, Inc., Lebanon, N. H., 03766, USA, 2006
[27] Pak, B. C., Cho, Y. I., Hydrodynamic and Heat Transfer Study of Dispersed Fluids with Submicron Metallic Oxide Particles, *Experimental Heat Transfer*, *11* (1998), 2, pp. 151-170
[28] Wang, X., *et al*., Thermal Conductivity of Nanoparticles-Fluid Mixture, *J. Thermophys. Heat Transfer*, *13* (1999), 4, pp. 474-480
[29] Patel, H. E., *et al*., A Micro-Convection Model for Thermal Conductivity of Nanofluid, *Pramana-J. Phys*, *65* (2005), 5, pp. 863-869
[30] Minea, A. A., Effect of Microtube Length on Heat Transfer Enhancement of a Water/Al_2O_3 Nanofluid at High Reynolds Numbers, *Int. J. Heat Mass Transfer*, *62* (2013), July, pp. 22-30
[31] Bouhalleb, M., Abbassi, H., Numerical Investigation of Heat Transfer by CuO-Water Nanofluid in Rectangular Enclosures, *Heat Transfer Engineering*, *37* (2016), 1, pp. 13-23
[32] Kakac, S., Pramuanjaroenkij, A., Review of Convective Heat Transfer Enhancement with Nanofluids. *Int. J. Heat Mass Transfer*, *52* (2009), 13-14, pp. 3187-3196
[33] Wang, X. Q., Mujumdar, A. S., Heat Transfer Characteristics of Nanofluids: A review, *Int. J. Therm. Sci*., *46* (2007), 1, pp. 1-19
[34] Rush, T. A., *et al*., An Experimental Study of Flow and Heat Transfer in Sinusoidal Wavy Passages, *Int. J. Heat Mass Transfer*, *42* (1999), 9, pp. 1541-1553

[35] Das, D., Arakeri, J. H., Transition of Unsteady Velocity Profiles with Reverse Flow, *J. Fluid Mech., 374* (1998), Nov., pp. 251-283
[36] Wang, S. P., Vanka, S. P., Convective Heat Transfer in Periodic Wavy Passages, *Int. J. Heat Mass Transfer*, *38* (1995), 17, pp. 3219-3230
[37] Saniei, N., Dini, S., Heat Transfer Characteristics in a Wavy Walled Channel, *Int. J. Heat Mass Transfer*, *115* (1993), 3, pp. 788-792

Paper submitted: October 18, 2016
Paper revised: October 23, 2016
Paper accepted: January 25, 2017